

# Supporting Material

## Appendix A

Pictures of apparent contact angles are presented for all studied conditions in the Figure 1.

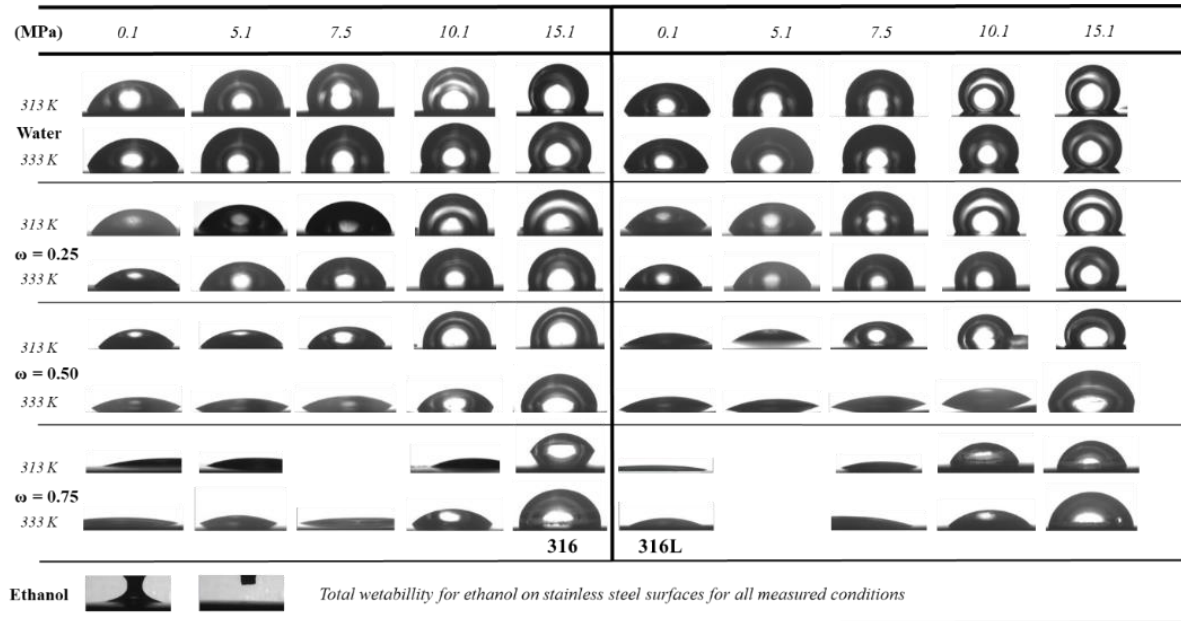


Figure 1 Apparent contact angles through all explored conditions

## Appendix B

Corrections of the apparent contact angles through the Wenzel equation are presented for various roughness parameters in the Figure 2.

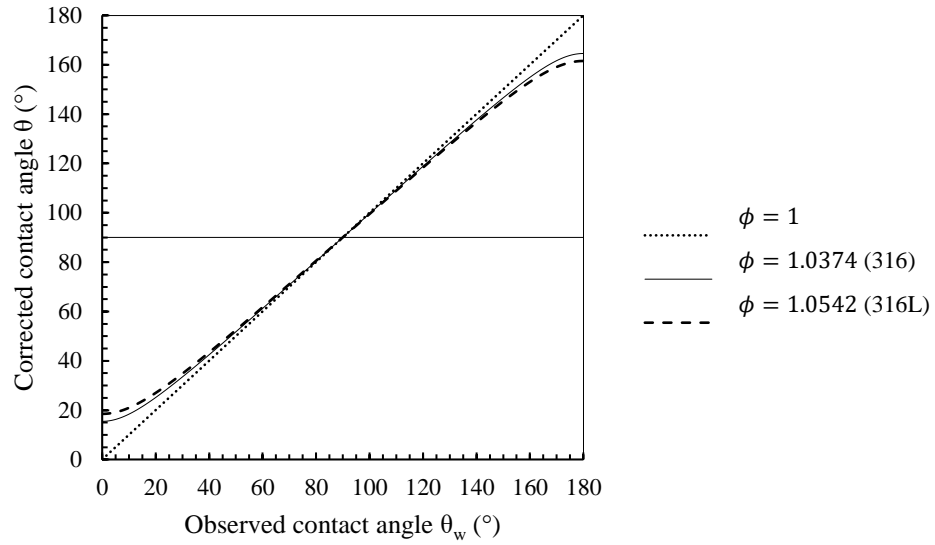


Figure 2 Roughness effect following the Wenzel equation considering maximal values of  $\phi$  parameter for AISI 316 and AISI 316L surfaces

## Appendix C

Table 1 and Table 2 regroup all averages of corrected contact angles obtained in this work with the statistical uncertainties calculated for a 95% confidence level. Each measurement was carried out at least in triplicate then corrected through the Wenzel equation and finally averaged.

Table 1 Data of corrected contact angle (CA) at 313.15 K for AISI 316 and AISI 316L with statistical uncertainties

P (MPa)	T (K)	$\omega_{\text{ethanol}}$	CA 316 (°)	CA 316L (°)
------------	----------	---------------------------	---------------	----------------

0.1	313.15	0	79	±	8	78	±	10
5.1	313.15	0	92	±	4	103	±	8
7.5	313.15	0	104	±	6	108	±	8
10.1	313.15	0	102	±	6	122	±	9
15.1	313.15	0	112	±	7	125	±	15
0.1	313.15	0.25	61	±	2	60	±	4
5.1	313.15	0.25	68	±	6	72	±	3
7.5	313.15	0.25	87	±	4	92	±	6
10.1	313.15	0.25	94	±	7	117	±	6
15.1	313.15	0.25	93	±	5	118	±	6
0.1	313.15	0.5	47	±	3	39	±	3
5.1	313.15	0.5	50	±	3	42	±	4
7.5	313.15	0.5	63	±	11	72	±	5
10.1	313.15	0.5	93	±	3	86	±	14
15.1	313.15	0.5	96	±	5	116	±	16
0.1	313.15	0.75	22	±	3	25	±	4
5.1	313.15	0.75	27	±	3			
7.5	313.15	0.75				27	±	3
10.1	313.15	0.75	33	±	4	64	±	9
15.1	313.15	0.75	62	±	3	82	±	6
0.1	313.15	1	0			0		
5.1	313.15	1	0			0		
7.5	313.15	1	0			0		

Table 2 Data of corrected contact angle (CA) at 333.15 K for AISI 316 and AISI 316L with statistical uncertainties

P (MPa)	T (K)	$\omega_{\text{ethanol}}$	CA 316 (°)			CA 316L (°)		
0.1	333.15	0	66	±	6	76	±	1
5.1	333.15	0	97	±	2	94	±	3
7.5	333.15	0	96	±	5	103	±	3
10.1	333.15	0	102	±	14	117	±	2
15.1	333.15	0	117	±	4	128	±	3
0.1	333.15	0.25	51	±	6	60	±	7
5.1	333.15	0.25	56	±	7	71	±	4
7.5	333.15	0.25	77	±	2	84	±	4
10.1	333.15	0.25	94	±	4	105	±	5
15.1	333.15	0.25	105	±	2	120	±	1
0.1	333.15	0.5	38	±	3	37	±	3
5.1	333.15	0.5	34	±	2	32	±	4
7.5	333.15	0.5	34	±	6	38	±	6
10.1	333.15	0.5	63	±	3	44	±	5
15.1	333.15	0.5	82	±	3	78	±	3
0.1	333.15	0.75	21	±	1	27	±	4
5.1	333.15	0.75	24	±	5			

7.5	333.15	0.75	26	±	4	29	±	3
10.1	333.15	0.75	53	±	5	47	±	2
15.1	333.15	0.75	75	±	3	77	±	4
0.1	333.15	1	0			0		
5.1	333.15	1	0			0		
7.5	333.15	1	0			0		
10.1	333.15	1	0			0		

## Appendix D

The ratio  $\gamma_{SF}/\gamma_{LF}$  of water at 313 K in saturated dense CO<sub>2</sub> as a function of pressure is presented in Figure 3. Data of  $\gamma_{SF}$  are taken from [52] and data of  $\gamma_{LF}$  are taken from [34].

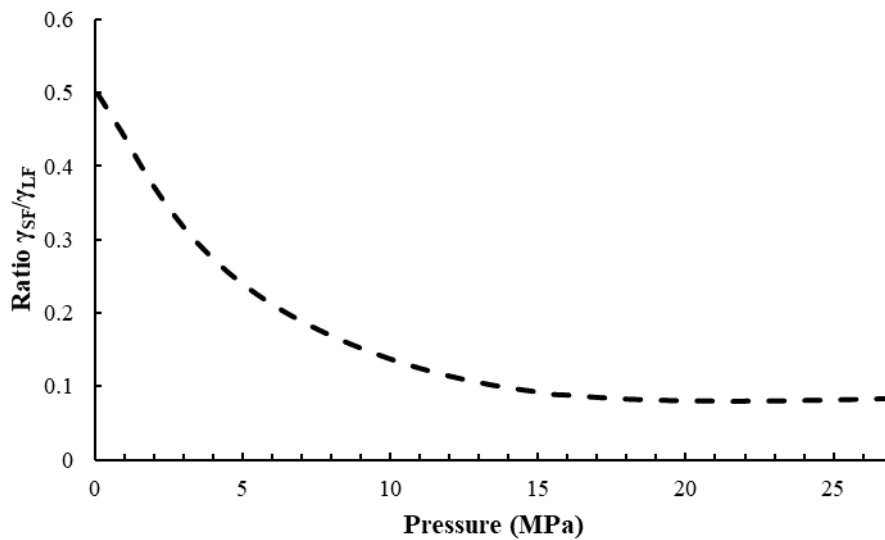


Figure 3 Ratio  $\gamma_{SF}/\gamma_{LF}$  as a function of pressure for CO<sub>2</sub>/water/ stainless steel system at 313 K, data used are from [52] for  $\gamma_{SF}$  and from [34] for  $\gamma_{LF}$

## Appendix E

Influence of the chemical heterogeneity of the solid/liquid interface for various arbitrary wetted fraction  $\sigma$  is presented in Figure 4.

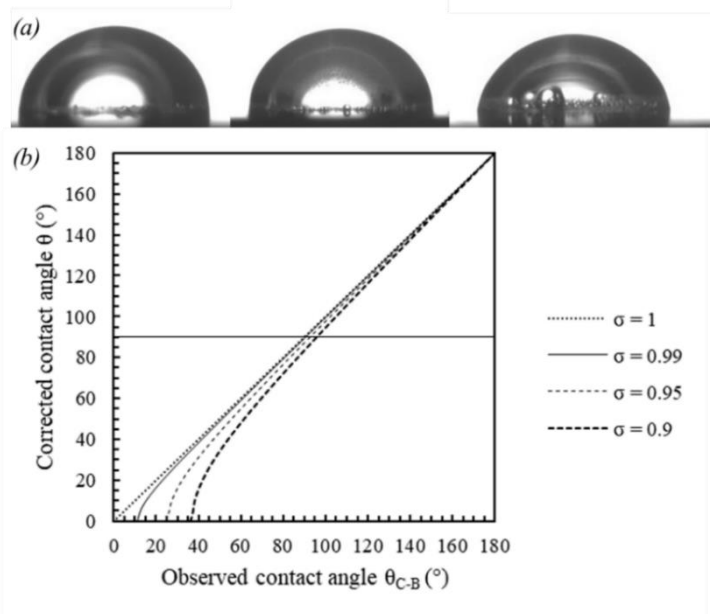


Figure 4 (a) picture of trapped bubbles, (b) correction of the observed contact angle through the Cassie-Baxter equation for various arbitrary wetted fraction